SYNTHETIC APERTURE RADAR IMAGES OF OCEAN WAVES, THEORIES OF IMAGING PHYSICS AND EXPERIMENTAL TESTS

John F. Vesecky, Stephen L. Durden,
Martha P. Smith and David A. Napolitano
Stanford Center for Radar Astronomy
Durand Building, Stanford University
Stanford, CA 94305 USA

1. INTRODUCTION

Observation of ocean surface waves was one of the primary reasons for including the synthetic aperture radar (SAR) in the instrument complement of the SEASAT oceanography satellite. As a natural result, understanding SAR response to ocean waves has been a central issue in the interpretation of SAR ocean images. Although much research has been done and several models have emerged to explain the mechanism for SAR imaging of ocean waves, only limited agreement has been reached on a correct understanding of the mechanism. Understanding the physics of this imaging mechanism is important for two reasons. First, understanding the imaging mechanism would allow improved estimates of wave field characteristics. Second, knowledge of the imaging physics for ocean gravity waves would have significant application to SAR images of other ocean surface phenomena, such as internal waves, slicks, surface wind fields and sea surface temperature variations. Our approach to understanding SAR imaging mechanisms is straightforward. First, we develop from each candidate model a set of hypotheses which can be experimentally tested. Second, we test these statements using data sets of SAR images and corresponding in situ surface observations. Our primary source of data sets has been from the SEASAT mission and several large scale field experiments using aircraft SAR's. This paper will summarize initial research results and the conclusions that can be drawn from them.

2. CONTENDING MODELS

Here we discuss three major models which claim to contain the important physics of the SAR imaging mechanism for ocean gravity waves. We pick these models because they represent major, different and well known points of view. Much of the physics involved here is relevant to other areas of ocean remote sensing by radar. While there are other important contributions to this problem (e.g. Swift & Wilson, 1979; Valenzuela, 1980; Ivanov, 1982 & 1983; Plant, 1983; Rotheram, 1983), we focus on work by Alpers et al (1981), Alpers (1983), Harger (1981 & 1984) and Jain (1981).

Two basic mechanisms for radar wave scattering from a statistically rough surface have been treated analytically. For a surface which is only slightly rough ($|k \zeta \cos\theta| \ll 1$, where k is radar wavenumber, ζ height deviation and θ angle of incidence) a perturbation analysis can be used and the resulting backscatter mechanism is referred to as the Bragg mechanism because of the analogy with Bragg (resonant) scattering from a crystal lattice. Here the structure resonant with the radar waves is a collection of short (~ 10's of cm) ocean waves. The other case is termed the quasi-specular mechanism since it evokes scattering from a statistical ensemble of facets, each scattering via specular reflection. This mechanism is valid for situations where ζ may be large, but the surface is gently undulating (radius of curvature >> radar wavelength). In general Bragg scatter is more impor-

137

tant for $\theta \gtrsim 20^0$ while quasi-specular scatter dominates for $\theta \lesssim 20^0$. In under-standing the models discussed below it is important to note the role played by each of these mechanisms. This is especially important for SEASAT SAR observations since $19^0 < \theta < 26^0$ in that case. Fig. 1 shows the observational geometry for SAR ocean remote sensing.
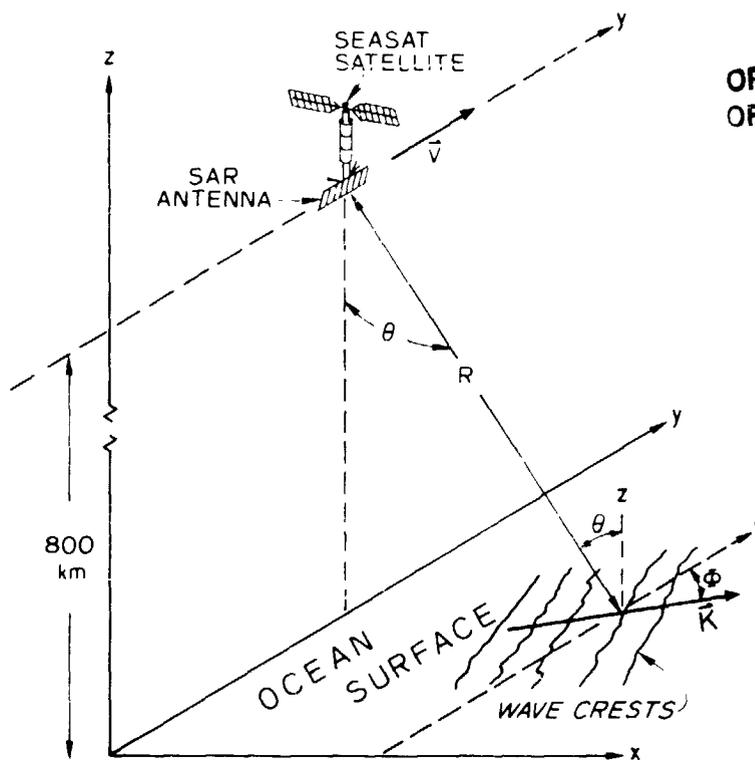
Fig. 1. Geometry for observation of the ocean surface by SEASAT (or aircraft) syn-thetic aperture radar. Here we define the geometry for SEASAT SAR observations of the ocean surface, (x,y) plane; in particular, observations of long gravity waves at a point (x,y) traveling at an angle Φ with respect to the SAR flight path and having a wave vector $\vec{K}$ where $K = (2\pi/\Lambda)$ and Λ is the ocean wave-length.

Alpers, et al. (1981-1983)

This model contains perhaps the most straightforward and easily comprehended analysis of SAR imaging of ocean waves. In this (ARR) model small ($\gtrsim 10$ radar wave-lengths) facets are treated as floating corks, each with its own Doppler shift and scattering properties. Each facet is statistically independent of surrounding fac-ets and a two-scale scattering model is used to calculate the radar echoes which determine the SAR image. The facets constitute the small scale, while the long (~ 10's to 100's of m) ocean waves determine the large scale surface behavior. So each facet has its own position, orientation, surface roughness and velocity. These properties are governed by the large scale, long ocean wave behavior. Given a fac-et's position, ocean surface dynamics determine the latter three quantities. Then, knowing a facet's orientation, surface roughness and velocity, Alpers et al use SAR and scattering theory to calculate the backscattered power which the SAR would sense from each facet location. Facet orientation, surface roughness and velocity vary with position along the propagation direction of a wave and give rise to three mech-

138

anisms by which a long ocean wave modulates the power sensed by the SAR for a given position along the wave propagation direction. This modulation makes the waves visible in the SAR image. Facet orientation leads to the tilt modulation mechanism in which, for a given surface roughness, the radar backscatter is enhanced when the long ocean wave tilts a facet so that it is viewed at nearer normal incidence by the radar and visa-versa. Facet roughness leads to the hydrodynamic modulation mechanism in which, for a given orientation, the radar backscatter is enhanced for those portions of a wave (near the crest) where surface dynamics enhances small scale roughness. Finally, facet velocity along the radar propagation vector $\vec{k}$ leads to the velocity bunching modulation mechanism in which, for a given tilt and surface roughness, the backscattered power sensed by the radar is systematically misplaced in the image due to the facet having a Doppler shift different from the mean for the large scale surface, i.e. Doppler misplacement bunches power in some image locations and disperses it from others. Alpers and Rufenach (1979), Alpers et al. (1981) and Alpers (1983a) apply this model to monochromatic sinusoidal waves while Alpers (1983b) uses a Monte Carlo calculation to make the application to a spectrum of waves. This model is relatively well developed and many quantitative statements which can be experimentally tested have been derived from it. Some of these statements are in terms of a modulation transfer function R defined by Alpers and Hasselmann (1979) as

$$ \sigma = \sigma_0 + \varepsilon\sigma = \sigma_0[1 + \int (R(K)\ z(K)\ e^{i(Kx-\Omega t)} + c.c.)\ dK] \qquad (1) $$

where σ is normalized radar cross section $z(K)$ is the Fourier transform of the surface height fluctuation associated with the long waves, K and Ω are the wavenumber and radian frequency of the long waves and c.c. stands for complex conjugate. Equation (1) implies that R characterzes a linear process. This is an unwarranted, but apparently useful assumption. R is of course a function of observational and ocean parameters as well as K. Since R relates SAR and ocean surface observables it can be determined experimentally and this empirically determined R compared with theoretical expressions from the different models. The model also makes predictions regarding other quantities, for example image smearing (degraded resolution) and biases of SAR estimates of wave characteristics relative to surface measurements. Because of the relatively straightforward connection between assumptions and predictions of this model we have emphasized it here.

Harger (1980-1984)

Harger (1980, 1981, 1983, 1984) approaches the SAR wave imaging problem from a radar point of view and his extensive background in SAR (e.g., Harger, 1970). In this model the ocean surface is characterized as a continuous, dynamic surface having an 'effective reflectivity density' (g) which varies spatially and temporally in accordance with the surface dynamics. Thus this model uses a distributed radar scattering surface rather than the floating corks of Alpers et al. The key elements in the model are SAR imaging of time variant scenes, rough surface scattering and ocean surface hydrodynamics. Harger (1980) characterizes the SAR system as a series of transformations in which $g(x,y)$ of the ocean surface [Fig. 1 coordinates are used here] is transformed into $I(x,y)$ which is the SAR image output. Harger (1980, 1981, 1983) investigates how these transformations filter the wavenumber spectrum of g to yield the wavenumber spectrum of I. To obtain g Harger (1984) uses Phillips' (1981) hydrodynamic model for short ocean waves (small scale roughness) riding on long gravity waves (large scale structure), i.e. a two scale model. The large scale waves are simple sinusoids. For scattering from small scale roughness the Bragg scattering model is used. In this imaging model, Phillips' hydrodynamic model produces hydrodynamic modulation analogous to, but not the same as, the work of Alpers et al. above. Tilt modulation is produced by the large scale

sinusoidal waves. There are several <u>major differences</u> between the results of this model and those of Alpers et al. <u>First,</u> Harger finds no 'velocity bunching' modulation effects whereas Alpers et al. do. <u>Second,</u> Harger finds the long wave phase velocity to be important whereas this quantity does not directly enter the model of Alpers et al.

Jain (1981)

This model is less fully developed than the previous two, but raises some important questions. Jain's model uses a distributed radar scattering surface as does Harger. He makes provision for quasi-specular as well as Bragg scattering and for scattering features travelling at the long wave phase velocity. Further he questions the application of the two scale model used by both Alpers et al. and Harger. While tilt and hydrodynamic modulation are included in this model, Jain and Harger agree that velocity bunching modulation should not be present. Jain's model is less well developed and quantitative predictions which can be experimentally tested are fewer. One prediction is that ocean wave fields containing wave trains in multiple directions will in general exhibit different properties than a simple super-position of two wave-train images rotated with respect to one another. Further Jain contends that for SAR observations at $\theta \lesssim 20^0$ (including SEASAT SAR) quasi-specular scattering is important. We discuss this question further below.

Key Issues

Here we summarize the major issues which we think are the crux of the wave imaging problem.
    1. <u>Role of surface motion:</u> Does a SAR sense radar scattering as having a Doppler <u>shift associated with the orbital or with the phase velocity</u> of an underlying long wavelength ocean wave? Is the velocity bunching mechanism valid?
    2. <u>Degradation of SAR resolution by ocean surface motion:</u> Is the degradation related primarily to long wave orbital acceleration (Alpers et al.) or does the presence of more than one dominant wave component imply a degradation of resolution as claimed by Jain?
    3. <u>Relative importance of quasi-specular, Bragg or other mechanisms:</u> Alpers et al. and Harger consider only Bragg resonant scatter. Is quasi-specular scattering also important as Jain claims? Within the Bragg mechanism what is the relative importance of the tilt, hydrodynamic and velocity bunching mechanisms?
    4. <u>Validity of the two-scale scattering model:</u> Can the ocean surface be separated into two importance scale lengths, the long ocean waves and the short Bragg resonant waves, as Alpers et al. and Harger assume or are intermediate scales also important as Jain claims?

3. RELEVANT EXPERIMENTAL DATA

There is a large collection of SAR and surface data sets concerning ocean waves. Several large field experiments were conducted both preceeding SEASAT (1978) and after, e.g., Marineland in 1975, Westcoast in 1976, and MARSEN in 1979. In these experiments various aircraft SAR's were flown over wave fields also observed by buoys, pressure arrays, wave staffs, and ground wave radar. Particularly useful are the multiple direction flights which view waves from several aspects. During the Seasat mission 100,000,000 km² of SAR images were collected, most over the ocean. The Seasat data have the advantage of a consistent SAR system and <u>very high quality digital imaging.</u> Several good data sets of SEASAT SAR and surface wave observations were collected during the JASON, GOASEX, DUCKEX, and Atlantic Coast experiments in 1978. Besides simple wavefields observed during the SEASAT mission there are several cases of ship wake waves and waves near islands which bear upon

the SAR ocean waves imaging mechanism. Two other sources of important experimental data are tower experiments, such as those of Plant (1977), and scaled down laboratory experiments. An extensive tower experiment called TOWARD will begin in August 1985 using the NOSC tower off San Diego. It will involve tower mounted radars, aircraft SAR and the Shuttle Imaging Radar, SIR-B. Other relevant wave experiments are planned for SIR-B in August 1984, in particular SAR observations at varying incidence angles (θ).

In bringing these data sets to bear on the SAR imaging problem two factors are of major importance. First, the SAR (or other radar) and surface and measurement data must test some critical hypothesis emerging from the contending models, i.e., the data set should address one of the critical issues listed above. Second, both the radar and surface data must be of sufficiently high quality to make a convincing test. In particular digitally imaged SAR data should be used whenever possible. Below we discuss some initial results using the aforementioned data sets to confront hypothesis derived from the models of section 2.

4. EXPERIMENTAL TESTS OF MODEL PREDICTIONS

Here we present initial results using data of section 3 to test the models of section 2. These results are limited both because this report is a brief one and because the research is still going on. The model of Alpers et al. receives somewhat more attention here because these authors have worked out a number of predictions which can be tested by available data in a straightforward manner.

Bias of SAR Estimates of Wave Properties Relative to Surface Measurements

One of the most straight forward comparisons of SAR estimates of wave properties with surface measurements is for the dominant wavelength of the ocean wave field being observed. Gonzalez et al. (1981) and Vesecky et al. (1983 and 1984) make such comparisons using SEASAT SAR data for several tens of cases.

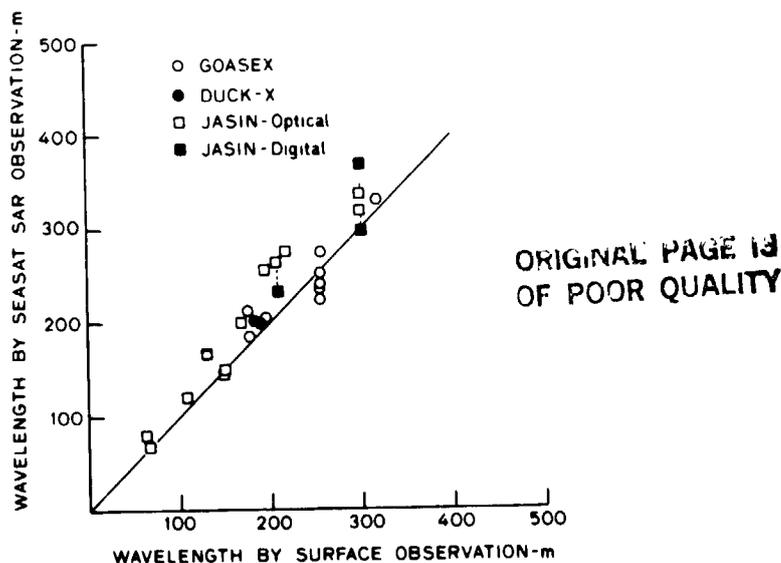

ORIGINAL PAGE IS
OF POOR QUALITY

Figure 2. Comparison of SAR and surface measurements of dominant ocean wavelength. Results are shown for optically produced SAR images in the GOASEX, JASIN and DUCK-X experiments. The black squares show some JASIN results using SAR images digitally produced at DFVLR and kindly provided by Dr. Werner Alpers, Max Planck Institute for Meterology, Hamburg.

141

Because the physical mechanism which allow SAR to image ocean waves are not well understood, first order estimates of ocean wave characteristics are based on a simple assumption, namely that intensity fluctuations, δI, in a SAR image of ocean waves are linearly proportional to fluctuations in ocean waveheight, $\delta\zeta$. Thus we let

$$F_I^2 = H^2 \, B^2 \, R^2 \, \Psi \tag{2}$$

where H is the transfer function related to the SAR system characteristics, B is related to oceanic background fluctuations not directly related to ocean waves, R is related to the physics of the wave imaging mechanism and F_I (K Φ) is the Fourier transform of the image intensity I(x,y) and K and Φ are polar coordinates in two-dimensional wavenumber space. The angle Φ is referenced to the velocity vector of the platform surface track and is positive clockwise when viewed from the platform. Thus $\Phi = 0$ is the azimuth or along track direction and $\Phi = 90$ is the range or cross track direction (see Fig. 1). The SAR wavelength estimates in Fig. 2 were made by computing F_I^2 from SAR images, letting B and R be unity and estimating the SAR system response H^2 according to Beal et al. (1983) for the JASIN digitally imaged data and according to Vesecky et al. (1984) for the JASIN optically processed data. For the GOASEX and DUCK-X optically processed data $H^2 = 1$. Thus biases due to SAR system response H^2 should be limited while biases due to the imaging mechanism R^2 remain. It is clear that the SAR estimates are biased slightly toward longer wavelengths. Monte Carlo simulations of SAR imaging of a spectrum of ocean waves by Alpers (1983) clearly predict such a bias (see Figs. 3, 7, 9, 10, 11, and 12). However, the parameters of these simulation do not match precisely the conditions of Fig. 2 (e.g., only the azimuthal component of the wave field is simulated). Hence, we can make only a semi-quantitive confirmation of this prediction of the Alpers et al. model. No analagous predictions for the Harger and Jain methods have been done so we can not evaluate them at this time.

Relative Importance of Bragg Resonance and Quasi Specular Scattering Mechanisms

It is well known (Bahar et al., 1983) that the relative importance of the Bragg resonance and quasi specular scattering mechanisms varies with angle of incidence (θ in Fig. 1). In section 2 we noted that both the Alpers et al. and Harger models take only Bragg scattering into account, while Jain contends that for the SEASAT SAR geometry specular scatter is also important. As a first step in sorting out this problem Vesecky et al.(1983) have calculated the variation of the modulation transfer function [R in eq. (1)] with incidence angle (θ). In this calculation only the tilt modulation mechanism was considered. In the calculation a SAR resolution wavenumber, $K_{sar} = \pi/(\text{resolution})$, is defined such that waves with $K < K_{sar}$ are imaged and waves with $K > K_{sar}$ are not. Waves that can be imaged are treated deterministically, while sub-resolution waves are treated statistically. Thus, the resolution cell is considered to be a random rough surface which is tilted by the deterministic long wave. To find the cross section in the resolution cell as a function of angle of incidence θ and the tilt angles, ψ and δ, a two-scale model is used. The height of the surface within the resolution cell is:

$$h = h_l + h_s \tag{3}$$

where h_s is for a small scale surface which scatters by the Bragg mechanism and h_l is for the large scale surface which scatters by the quasi specular mechanism. Here large scale refers to waves intermediate between the Bragg resonant wavelength ($\sim$30 cm) and the resolution cell size ($\sim$25 m). The waveheight spectrum for h is derived into three parts:

142

$$W(K) = \begin{cases} W_s\,(K) & K > D_d \\ W_1\,(K) & K_{SAR} < K < K_d \\ 0 & K < K_{SAR} \end{cases} \qquad (4)$$

k_d is the wavenumber of transition between the large scale surfaces.

In Fig. 3 results are shown for three progressively complex model calculations. In the most simple case (dotted line) quasi specular is neglected as well as the tilting of h_s by h_1. This corresponds to the Alpers et al. model and is the same curve as Fig. 1 of Alpers et al. (1981). Next the tilting of h_s by h_1 is included, but only Bragg scatter is considered. This corresponds, at least in part, to including the effects of surface height structure in between the small scale Bragg resonant waves (~30 cm) and the long ocean waves (~100's of m). These results corresponding to the dashed line go toward zero at small θ as one knows physically they should. Finally quasi-specular scatter is included (solid curve) and a peak in the modulation transfer function emerges at $\theta \sim 18°$. Similar results have been obtained by Bahar et al. (1983).
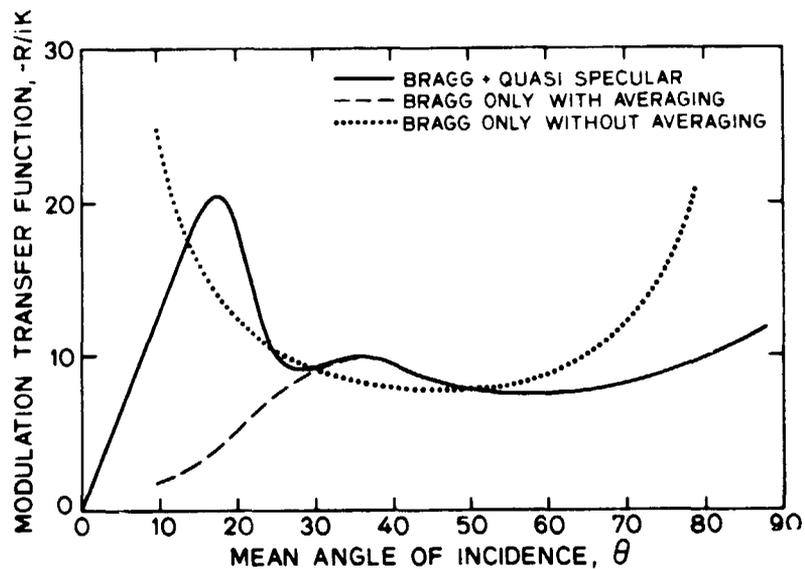
Fig. 3. Normalized modulation transfer function (-R/ik) taking into account various effects.

According to Fig. 3 one should observe a rather sharp decline in the visibility of waves in SAR images as θ increases from about 20° to 30°. SEASAT SAR observations over the JASIN experiment area off the west coast of Scotland provide an opportunity to test this implication of Fig. 3. On orbit 1044 300 m wavelength waves at $H_{1/3} \sim 3.5$ m traveling at about 40° relative to the satellite surface track ($\Phi \sim 229°$ in Fig. 1) were imaged by SEASAT SAR. A scene about 40 x 40 km in size was digitally imaged at DFVLR Oberpfaffenhofen. This image was divided into 9 squares -- 3 in azimuth by 3 in range. Along the range direction θ varies over a little less than 2°. SAR estimates for Ψ were obtained as discussed above letting R^2 and B^2 go to unity in eq. (2). The relative values of the Ψ estimates at the dominant wavenumber K_p were compared to note the variation of SAR estimate of

143

$\Psi(\vec{K}_B)$ with θ. If one assumes that the ocean wavefield is homogeneous over the 40 x 40 km square, that SAR system effects have been successfully removed, and that there are no relevant background contributions (e.g. from internal waves), then the variation must be due to R^2 in eq. (2), i.e. to the imaging mechanism. Over this 40 x 40 km area 300 m swell in deep water should be very nearly homogeneous even in the 11 m/s wind blowing at the time. Use of H^2 in eq. (2) as discussed above, plus the fact that we are considering wave sizes much smaller than the image size and that the digital imaging was carefully done convince us that the variation seen in Fig. 3 is not due to SAR or imaging artifacts. Further visual examination of the image reveals no significant background effects. Thus although this initial result must be confirmed from other data, we think it is indicative of a real variation of R^2 with θ and thus can be considered as experimental evidence confirming the existence of a rapid decrease of R^2 with θ for $20° \lesssim \theta \lesssim 30°$. Knowing the origin of Fig. 3 we thus have experimental evidence for the importance of quasi-specular scattering for SEASAT SAR images of ocean waves.
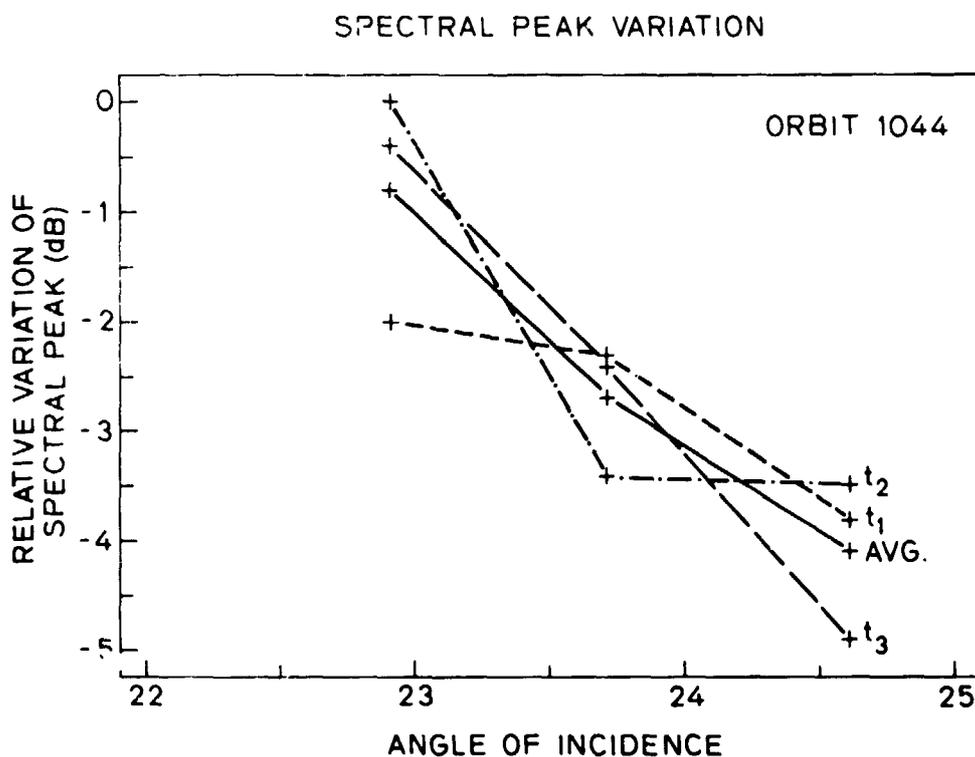
SPECTRAL PEAK VARIATION

Fig. 4. Dependence of the SAR estimate of the directional wave spectrum Ψ (at the dominant wavenumber) on incidence angle θ. The data comes from a 40 x 40 km SEASAT SAR image collected on orbit 1044 over the JASIN experiment area 8 Sept. 1978, 0019 GMT. The three curves correspond to deviding the image into a 3 x 3 matrix and calculating the θ variation (along the range direction) at three locations along the azimuth direction. The mean curve for the three is also shown.

Ship Wakes

SAR images of ship wakes take many forms as shown by Fu & Holt (1982) and Vesecky & Stewart (1982). Those images are not useful here because there were no corresponding surface wave measurements. However, in Fig. 5 we show a splendid

SEASAT image of a classical Kelvin ship wake. Since we can clearly identify the SAR image as a Kelvin wake and since we know a good deal about Kelvin wakes (e.g. Lighthill, 1978, ch. 3), some useful information can be obtained. Aside from its form, a very convincing argument that the wake is indeed a Kelvin wake was pointed out to the authors by Brian Barber of the Remote Sensing Centre, RAE Farnborough, U.K. Noting the displacement of the ship from the wake and the SAR observational parameters a speed of about 11 m/s can be calculated for the ship. From wake theory we know that the transverse waves in the wake must have a phase velocity equal to the ship's velocity. We can calculate the required wavelength of the transverse waves in the image. The wavelength observed in the image is within 10% of the required value.

The important point here is that the ship is displaced from the wake by an amount which implies that the wake is virtually stationary on the sea surface. We make the analogy with the familiar 'train off the track' phenomena of SAR images in which the train's motion displaces it from the stationary track because the train and track have different Doppler shifts and SAR uses Doppler shift to locate objects along directions parallel to the SAR flight path. Thus the SAR observes these ~90 m waves of the ship wake as if they were stationary with respect to the sea surface (as assumed by Alpers et al.) rather than as if they were moving at the wave phase velocity. A similar point was noted by Keith Raney in his lecture at the Royal Society Meeting on Remote Sensing in Autumn, 1982.
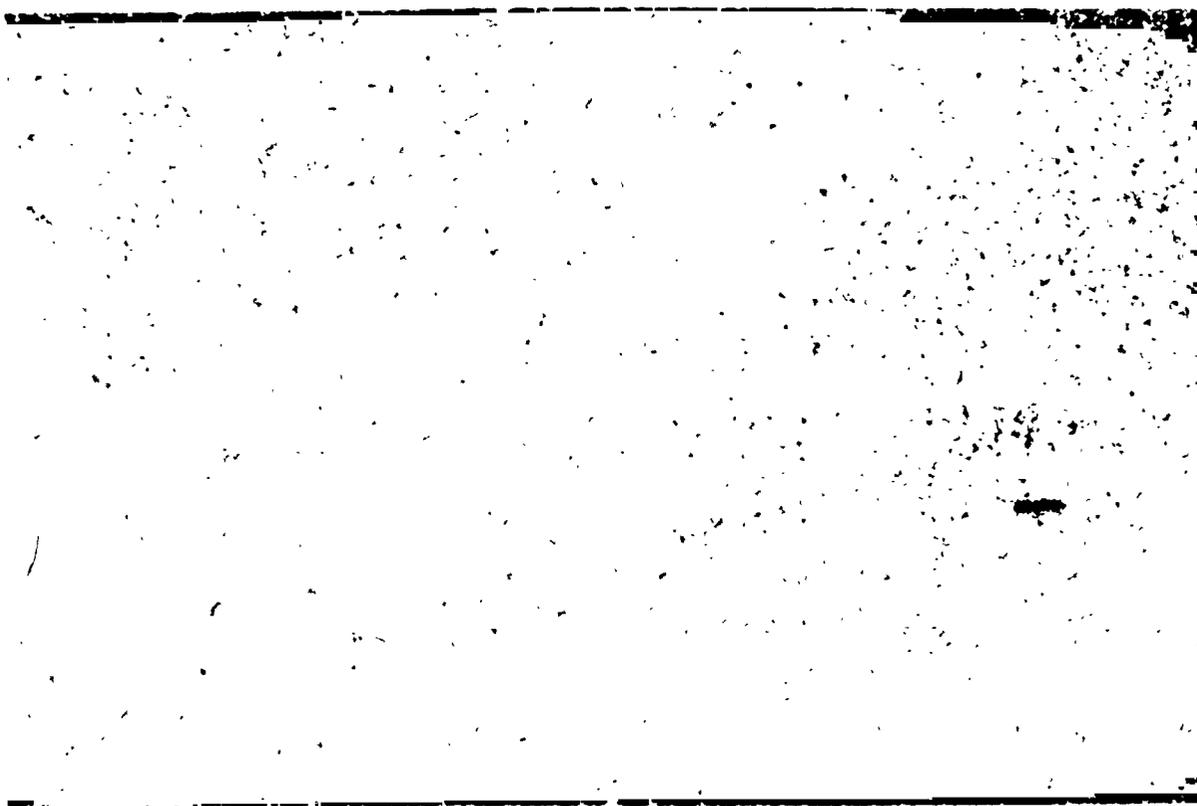

Fig. 5. SEASAT SAR image of a classical Kelvin wake generated by a ship in the English Channel. THe image was collected on orbit 834, 24 August 1978, at 0727 GMT and digitally image at the Remote Sensing Center, RAE Farnborough, U.K.

Conclusions

We have discussed three major models for the mechanism by which SAR images ocean waves. From section 2 we conclude that there are significant fundamental differences between these models. These differences occur both in fundamental assumptions and in subsequent developments. Thus it is not surprising to find significant differences between predictions arising from these different models. In section 2 we list four key issues which need to be resolved in order to sort out the correct and incorrect features in the contending models. Although testing these models against experimental evidence is still in the initial stages, we draw several preliminary conclusions. For the most part these conclusions require further testing to confirm them.

1. SAR estimates of dominant ocean wavelength are biased slightly toward longer wavelengths when compared to surface measurements. The work of Alpers (1983) predicts just such a bias. However, we have not yet made detailed quantitative comparisons.

2. Inclusion of the quasi-specular scattering mechanism (Fig. 3) produces predictions which appear to agree with experimental evidence (Fig. 4) regarding the variation of the modulation transfer function with angle of incidence. Hence the quasi specular scattering mechanism is important for SEASAT SAR observations ($\theta \sim 22°$) of ocean waves.

3. For the waves of the Kelvin ship wake of Fig. 5 the Doppler shift sensed by the SEASAT SAR is essentially that of the mean sea surface. Hence for these 90 m wavelength waves we conclude that wave orbital velocity is involved rather than wave phase velocity.

Future experiments using the Space Shuttle imaging radar (SIR-B) should be very helpful in resolving the key issues of section 2 both because observations will be made at multiple angle of incidence and because high quality digitally imaged data will be available. SIR-B observations during the TOWARD (instrumented sea tower) experiment off San Diego would be particularly useful.

REFERENCES

Allen, T.D. (ed.), 1983: Satellite Microwave Remote Sensing, Ellis Horwood, Chichester, U.K.

Alpers, W.R., 1983a: Imaging ocean surface waves by synthetic aperture radar -- a review, 107-120, in Allen (1983).

Alpers, W.R., 1983: Monte Carlo simulations for studying the relationship between ocean wave and synthetic aperture radar image spectra, J. Geophys. Res., 88, 1745-1759.

Alpers, W.R. and C.L. Rufenach, 1979: The effect of orbital motions on synthetic aperture radar imagery of ocean waves, IEEE Trans. Antennas and Propagat., AP-27, 685-690.

Alpers, W.R., D.B. Ross, and C.L. Rufenach, 1981: On the detectability of ocean surface waves by real and synthetic aperture radar, J. Geophys. Res., 86, 6481-6498.

Bahar, E., C.L. Rufenach, D.E. Barrick and M.A. Fitzwater, 1983: Scattering cross section modulation for arbitrarity oriented composite rough surfaces: Full wave approach, Radio Sci., 18, 675-690.

Beal, R.C., D.G. Tilley and F.M. Monaldo, 1983: Large- and small-scale spatial evolution of digitally processed ocean wave spectra from SEASAT synthetic aperture radar, J. Geophys. Res., 88, 1761-1778.

Fu, L-L and B. Holt, 1982: Seasat Views Oceans and Sea Ice with Synthetic-Aperture Radar, JPL Publ. 81-120, Jet Propulsion Lab., Pasadena, CA.

Gonzalez, F.I., R.A. Shuchman, D.R. Ross, C.L. Rufenach and J.F.R. Gower, 1981: Synthetic aperture radar observations during GOASEX, in Oceanography from Space, J.F.R. Gower (ed.), 459-468, Plenum Press, N.Y.

Harger, R.O., 1983: A sea surface height estimator using synthetic aperture radar complex imagery, IEEE J. Oceanic Engr., OE-8, 71-78.

Harger, R.O., 1981: Sar ocean imaging mechanisms, in Spaceborne Synthetic Aperture Radar for Oceanography (R.C. Beal et al., ed.), Johns Hopkins Press, Baltimore, 110-127.

Harger, R.O., 1984: The SAR imaging of short gravity waves on a long gravity wave, Proceeding of the IUCRM Symposium on Wave Dynamics and Radio Probing of the Ocean Surface (O.M. Phillips, ed.) Plenum Press, N.Y. (in press).

Harger, R.O., 1980: The synthetic aperture radar image of time-variant scenes, Radio Sci., 15, 749-756.

Harger, R.O., 1970: Synthetic Aperture Radar Systems, Academic Press, N.Y.

Ivanov, A.V., 1983: On the mechanism for imaging ocean waves by synthetic aperture radar, IEEE Trans. Ant. & Propagat., AP-31, 538-541.

Ivanov, A.V., 1983: Reply to "Comments on 'On the synthetic aperture radar imaging of ocean surface waves'" by W.J. Plant, IEEE J. Ocean Engr., OE-8, 300.

Ivanov, A.V., 1982: On the synthetic aperture radar imaging of ocean surface waves, IEEE J. Ocean Engr., OE-7, 96-102.

Jain, A., 1981: SAR imaging of ocean waves: Theory, IEEE J. Ocean Engr., OE-6, 130-139.

Lighthill, J.A., 1978: Waves in Fluids, Cambridge Univ. Press, Cambridge, U.K.

Plant, W.J., 1983: Comments on "On the synthetic aperture radar imaging of ocean surface waves", IEEE J. Ocean Engr., OE-8, 300.

Plant, W.J., 1977: Studies of backscattered sea return with CW dual-frequency X-band radar, IEEE Trans. Antennas and Propagat., AP-25, 28-36.

Rotheram, S., 1983: Theory of SAR ocean wave imaging in Allen (1983), pp. 155-186.

Swift, C.T. and L.R. Wilson, 1979: Synthetic aperture radar imaging of moving ocean waves, IEEE Trans. Ant. & Propagat., AP-27, 685-689.

Valenzuela, G.R., 1980: An asymptotic formulation of the SAR images of the dynamical ocean surface, Radio Sci., 15, 105-114.

Vesecky, J.F. and R.H. Stewart, 1982: The observation of ocean surface phenomena using imagery from the SEASAT synthetic aperture radar, J. Geophys. Res., 87, 3397-3430.

Vesecky, J.F., H.M. Assal and R.H. Stewart, 1981: Remote sensing of the ocean wave height spectrum using synthetic-aperture-radar images, in Oceanography from Space (J.F.R. Gower, ed.) Plenum Press, N.Y., 449-568.

Vesecky, J.F., S.L. Durden, D.A. Napolitano and M.P. Smith, 1983: Theory and practice of ocean wave measurement by synthetic aperture radar, Proceedings of Oceans '83, IEEE Press, N.Y.

Vesecky, J.F. R.H. Stewart, R.A. Shuchman, H.M. Assal, E.R. Kasischke and J.D. Lyden, 1984: On the ability of synthetic aperture radar to measure ocean waves, Proceedings of IUCRM Symposium of Wave Dynamics and Radio Probing of the Ocean Surface, (O.M. Phillips, ed.) Plenum Press, N.Y. in press.